

Energetics, structure, and long-range interaction of vacancy-type defects in carbon nanotubes: Atomistic simulations

J. Kotakoski,¹ A. V. Krasheninnikov,^{1,2} and K. Nordlund¹

¹*Accelerator Laboratory, University of Helsinki, P.O. Box 43, Helsinki FI-00014, Finland*

²*Laboratory of Physics, Helsinki University of Technology, P.O. Box 1100, Helsinki FI-02015, Finland*

(Received 6 October 2006; revised manuscript received 2 November 2006; published 15 December 2006)

The presence of vacancy clusters in carbon nanotubes has been assumed to explain the formation of carbon peapods and the difference between the experimentally measured and theoretical fracture strength of nanotubes. We use atomistic simulations at various levels of theory to study the characteristics of large vacancies formed by up to six missing atoms. We show that the formation of big “holes” on nanotube walls is energetically unfavorable as the vacancies tend to split into smaller defects due to the reconstruction of the nanotube atomic network. We also demonstrate that there is a weak but long-ranged interaction between the vacancies not only through strain fields but, surprisingly, also due to electronic effects, similar to those of adatoms on metal surfaces.

DOI: [10.1103/PhysRevB.74.245420](https://doi.org/10.1103/PhysRevB.74.245420)

PACS number(s): 81.07.De, 73.22.-f, 81.05.Tp

I. INTRODUCTION

Although single-walled carbon nanotubes (SWNTs) are frequently referred to as perfect crystalline wires, even high-quality nanotubes have at least one defect per each 4 μm .¹ Among them, single- and multiatom vacancies are some of the most prolific and important point defects. Vacancies can impede the adsorption of quantum gases on nanotube bundles,² govern the conductance of nanotubes,^{3–5} and control the operation of nanotube-based chemical sensors.⁶ They can also improve on the catalytic characteristics of nanotubes for thermal dissociation of water.⁷ Single vacancies and small vacancy clusters have been found to decrease the tensile strength and critical strain of nanotubes.^{8–10} Reconstruction of vacancies due to dangling bond saturation gives rise to many interesting effects, such as pressure buildup inside irradiated nanotubes,¹¹ nanotube welding,^{12,13} and coalescence.¹²

Not surprisingly, the structure and energetics of vacancies in nanotubes have been studied at length.^{14–19} However, the properties of nanotubes with vacancy clusters have received much less attention, although vacancy clusters have been thought to be highly important for understanding the carbon peapod formation process^{20,21} and the difference between the experimentally measured and theoretical fracture strength of nanotubes.⁸

In this work, we theoretically study the structure and energetics of vacancy clusters formed by removing 1–6 atoms from a nanotube. We calculate the formation energies of both metastable and the lowest-energy structures and estimate the energy gained when these defects are formed from single vacancies. We show that the formation of small vacancy clusters from single vacancies is energetically favorable in contrast to big “holes,” as the vacancies formed by more than five missing atoms tend to split into smaller defects. To fully understand the vacancy coalescence mechanism, we also study the long-range interaction between single vacancies through strain fields and electronic degrees of freedom.

II. METHODS

In our simulations, we used primarily a nonorthogonal density-functional-theory-based tight-binding (DFTB) mod-

el.²² In this approach the parameters of the Hamiltonian are derived from *ab initio* density-functional theory (DFT) calculations. The properties of point defects in nanotubes and graphite, as given by this method, have been shown to be in excellent agreement with those obtained by DFT calculations.^{17,23} The structural relaxation was done with an accuracy of 2.7 meV in the total energy.

To study long-ranged effects, we also used an empirical potential (EP) model of Brenner.²⁴ This model has been developed to describe carbon in both the graphite and diamond phases as well as a wide range of small carbon and hydrocarbon molecules. It has previously been widely used to study carbon nanotubes,^{8–10,25–29} in particular, it has been found to give the correct structure of mono- and divacancies in nanotubes²⁷ (although the latest modification of the potential³⁰ predicts that the lowest-energy configuration is a structure with a four-coordinated carbon atom, which is obviously incorrect).

Finally, for accurate calculations of the electronic structures of defected nanotubes, we employed DFT implemented in the plane wave basis set VASP code,³¹ with simulation setup similar to that used in previous calculations.^{17,32} In particular, we used projector augmented wave potentials³³ to describe the core electrons and the generalized gradient approximation³⁴ for exchange and correlation. All structures were fully relaxed until the forces acting on atoms were less than 20 meV/Å. A kinetic energy cutoff of 400 eV was found to converge the total energy of our system to within meV. The same accuracy was also achieved with respect to the \mathbf{k} -point sampling of the Brillouin zone (normally nine points along the tube axis).

The simulated nanotubes consisted of 100–600 atoms and had lengths of 12.3–36.9 Å (corresponding to 5–15 unit lengths for an armchair carbon nanotube). Much larger systems were used in EP calculations. The effect of finite system size was ensured to be negligible by repeating several calculations with significantly larger system sizes.

III. RESULTS AND DISCUSSION

We first calculated the structure and characteristics of 30 different vacancies by structural relaxation of the system

TABLE I. Formation energies of the vacancy structures calculated with the DFTB method. Values in parentheses give the number of atoms in carbon rings in defects. Subscripts show the number of dangling bonds in each ring. Orientations of defects (“parallel” \parallel and “perpendicular” \perp) are given as the orientation of the longest chain of missing atoms in each defect with respect to the nanotube axis.

Defect structure	Graphene	$E^{(f)}$ (eV)	
		(10,10)	(5,5)
$V_1(5-9_1)^\perp$	7.38	6.51	5.30
$V_2(5-8-5)^\parallel$	7.52	5.25	4.03
$V_2(5-5-5-7-7-7)$		6.24	
$V_2(5-8-5)^\perp$		8.22	7.72
$V_3(5-10_1-5)^\parallel$	10.67	8.70	6.77
$V_3(5-10_1-5)^\perp$		10.42	8.70
$V_4(5-7-7-5)^\parallel$	14.07	7.67	6.37
$V_4(5-7-7-5)^\perp$		9.04	
$V_4(5-5-5-9)$		10.32	
$V_5(5-5-5-11_1)$	14.94	11.27	9.06
$V_5(5-14_3-5)$		12.55	
$V_6(5-7-6-7-5)^\parallel$	19.58	7.68	6.68
$V_6(5-7-6-7-5)^\perp$		9.42	7.61
$V_6(5-7-6-7-5)^\perp$		13.27	
$V_6(18_6)$		17.21	

with the DFTB method. The defects were formed by removing 1–6 atoms from a pristine lattice with different atomic positions so that all possible configurations for the smallest vacancy clusters and the most likely configurations for the larger clusters (4–6 missing atoms) were included. We also considered some structures which can be obtained from the multivacancies by rearranging the atoms, as for example, the $V_2(5-5-5-7-7-7)$ defect³⁵ related to the double-vacancy [$V_2(5-8-5)$] defect; the numbers stand for nonhexagonal rings present in the system. In our previous studies,³⁶ we ran molecular dynamics simulations for defected nanotubes, but did not observe formation of any other low-energy structures. Formation energies $E^{(f)}$ of various stable and metastable configurations are presented in Table I, and the atomic structures of several defects are shown in Fig. 1. For single and divacancies, the calculated formation energies are in a very good agreement with the published data.^{14,17}

Atoms in the neighborhood of a vacancy defect reconstruct to saturate the dangling bonds if possible (see Fig. 1), similar to the vacancy behavior in graphene.^{35,37,38} The curvature allows the reconstruction to be stronger in nanotubes, shortening the bonds and locally decreasing the diameter of the SWNT. Due to the curvature, the minimum-energy structures for multivacancies in graphene and nanotubes may differ. For example, the lowest-energy configuration of a divacancy in a (10,10) SWNT is $V_2(5-8-5)$, in contrast to $V_2(5-5-5-7-7-7)$ reported for graphene.³⁵ Depending on the tube diameter, the difference in energy proved to be 0.6–1 eV, which is in agreement with the DFT result (0.7 eV) for a (5,5) SWNT.¹⁹

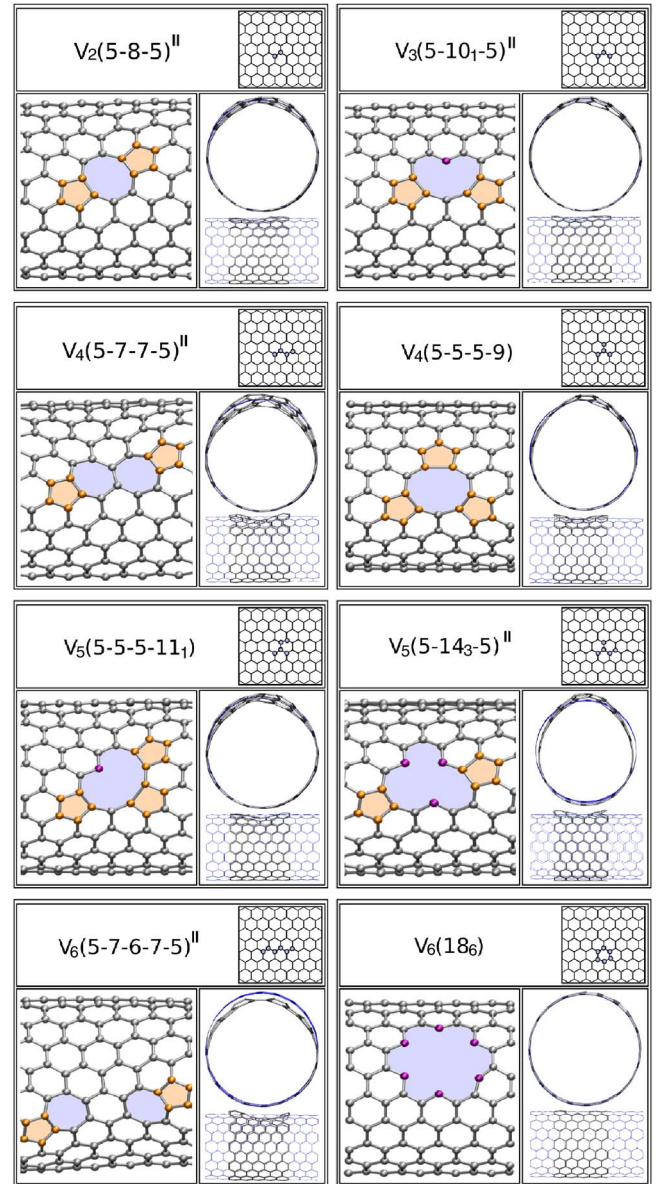


FIG. 1. (Color online) Atomic structures of multivacancies on a (10,10) SWNT given by the DFTB method. Pentagons are colored in yellow (light gray), rings with more than six atoms in blue (slightly darker gray). Atoms with dangling bonds are represented as red (dark gray) balls. The atomic network of the pristine tube with the removed atoms is shown in the top right corner of each panel. The right part illustrates changes in the nanotube network.

The lowest-energy structure for a tetravacancy in armchair nanotubes $V_4(5-7-7-5)^\parallel$ is also different from $V_4(5-5-5-9)$, which has the lowest energy in graphene.³⁷ Due to local shrinkage, the bonds perpendicular to the nanotube axis can shorten more easily, and therefore the energetically favored structures in nanotubes are those with the maximum number of perpendicular bonds. In graphite the circular structures are preferred because the stress can be shared in all directions on the plane.

The minimum-energy structure of a hexavacancy consists of two (5-7) defects separated by a perfect hexagon (see Fig. 1). The vacancy splits into two smaller defects accompanied

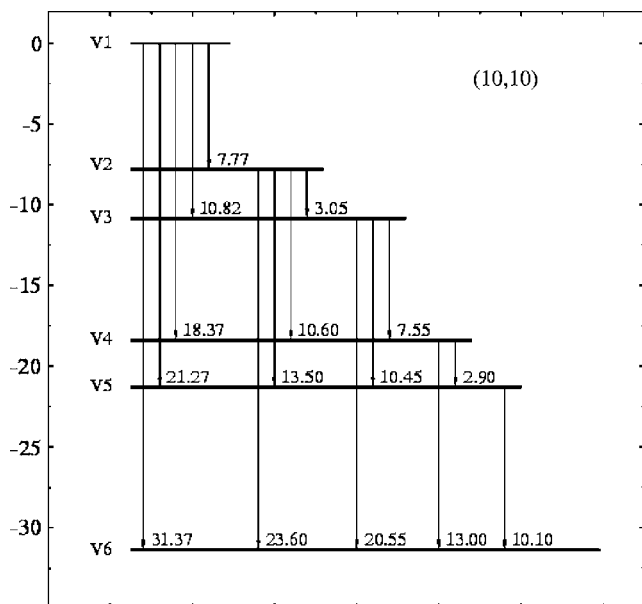


FIG. 2. Energies (in eV) gained by coalescing monovacancies (V_1) to form higher-order defects (V_i) on a (10,10) SWNT, as given by the DFTB method.

by a strong reconstruction of the nanotube atomic structure. As the difference in $E^{(f)}$ between this structure and the circular $V_6(18_6)$ defect is nearly 10 eV on a (10,10) SWNT, it can be inferred that multivacancies formed by six or more missing atoms tend to split into smaller vacancies instead of growing. For multiwalled nanotubes the effect should be weaker due to lower curvature. Higher-order defects can still be formed by removing a group of atoms at once with high-energy impacts or chemical etching, especially with hydrogen termination. However, these defects can be expected to reconstruct into chainlike defects by migration of the undercoordinated atoms to saturate the dangling bonds, thus closing the holes. Note that pressure buildup inside irradiated nanotubes^{11,39} could not occur if big vacancy clusters were energetically favorable.

As multivacancies can be formed from migrating single vacancies (for example, under electron irradiation^{11,36}), we also calculated the energy gained due to the coalescence of single vacancies into larger defects (see Fig. 2). The structures without dangling bonds (i.e., the ones with an even number of missing atoms) are clearly energetically the most favored; it costs less than 3.0 eV to add a single vacancy to odd-numbered multivacancies, whereas the energy needed to remove an atom from an even-numbered vacancy is more than 7.5 eV.

Because interaction between vacancies can affect their migration and coalescence, we studied in detail the effect of a vacancy on the nearby defects. Only single vacancies in nanotubes are mobile (the migration energy for a single vacancy in SWNTs is around 1.5 eV,¹⁷ while for a divacancy the migration energy is around 5 eV), so that we limited our simulations to single vacancies.

We created two single vacancies in a (5,5) SWNT at different positions along the tube axis and circumference with several orientations, fully relaxed the atomic structure, and

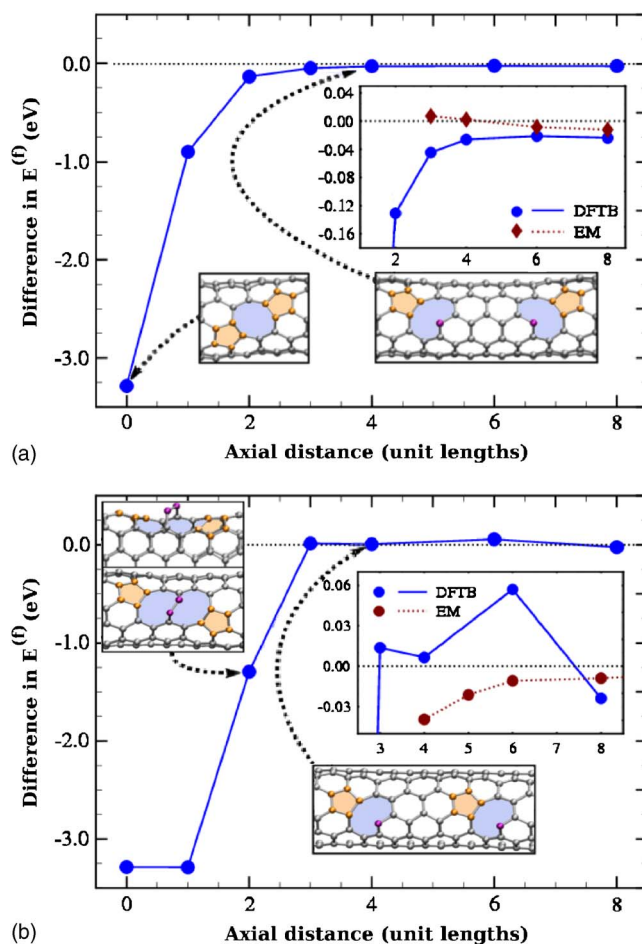


FIG. 3. (Color online) Difference in the vacancy formation energy in a (5,5) nanotube (two single vacancies) as a function of separation between the defects for two orientations as calculated with the DFTB method. The insets show the energy at large separations as calculated with both the DFTB and EP models. The arrows visualize the correspondence between the plot points and the atomic structures.

calculated the difference in the total energy with respect to the infinite separation between the defects as a function of the distance between the vacancies. The difference in vacancy formation energy $E^{(f)}$ (the same as the difference in the total energies) as a function of vacancy separation is shown in Fig. 3. When two vacancies are oriented along the tube axis, the energy goes down at small separations. The metastable defect configuration shown in the upper left corner in Fig. 3(b) was also found in graphene,⁴⁰ although in the case of nanotubes the curvature resulted in the elevation of two C atoms.

The results clearly indicate that there is a long-ranged interaction between the vacancies in the 10 meV range, which can be either attractive or repulsive. Qualitatively similar results were obtained for several different orientations of the vacancies. Interestingly enough, for some orientations of the vacancies, we found a nonmonotonic (sawtooth) dependence of the energy on the defect separation.

Simulations with the EP model gave qualitatively the same results as with the DFTB method at small separations

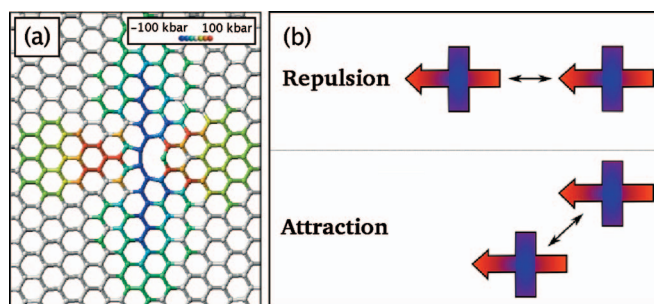


FIG. 4. (Color) (a) Strain fields near a single vacancy in graphene as given by the EP method. (b) Sketch illustrating the effect of vacancy orientation on the type of the interaction (repulsive or attractive) between two single vacancies in graphene.

between the vacancies, but the dependencies at large distances were different. As the interaction can originate from the overlap of the strain fields created by each defect, to understand the origin of the interaction, we computed the local pressure on atoms near a vacancy by evaluating the virials⁴¹ with the EP model. We considered a graphene sheet, and nanotubes with various chiralities. We found that two separate strain fields surround a single vacancy (see Fig. 4). The first field corresponds to the region where the bonds are shortened due to a new bond at the pentagon (blue and cyan atoms). The second field, oriented perpendicular to the first one, corresponds to the region where the bonds are stretched (yellow and red atoms). In nanotubes the fields are mixed and have shorter ranges due to the curvature-enhanced structure relaxation in the transverse direction. A partial compensation of the strain (and thus gain in energy when strain fields with opposite signs overlap) results in attraction between the vacancies, while the overlap of the fields of the same sign gives rise to repulsion.

Overall, we found a qualitative agreement between the results obtained with both DFTB and EP methods, except for the areas with energy oscillations found in the DFTB model. Careful analysis of the electronic structure of the SWNT with a single vacancy revealed that the energy oscillations come from the standing electron waves at the Fermi energy near the vacancy, as predicted earlier⁴² and experimentally confirmed⁴³ for nanotubes with irradiation-induced defects.

To get more insight into the electronic structure, we calculated the spatial distribution of the electron density in the energy range of 0.3 eV near the Fermi level with the DFT method. The results are presented in Fig. 5. The clearly observable electronic superstructure near the defect results in a nonmonotonic vacancy-vacancy interaction, as a slightly different amount of electron density is available for making a new bond at the pentagon of the second vacancy. A similar phenomenon—substrate-mediated long-ranged oscillatory interaction—was previously reported for adatoms on metal surfaces.⁴⁴ However, this result is somewhat unexpected for carbon nanotubes with a relatively small density of states at the Fermi level. Moreover, our simulations⁴⁵ indicate that there exists an electronic interaction between defects in not only metallic but also semiconducting nanotubes. As individual vacancy gives rise to a peak in the density of states

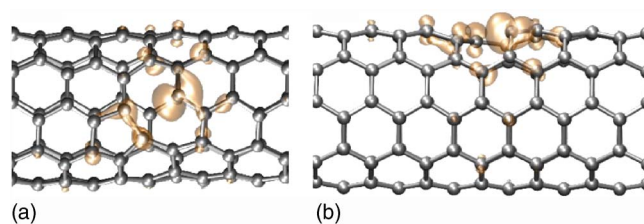


FIG. 5. (Color online) Isometric plot of the electron density near the Fermi level around a single vacancy in a (5,5) SWNT, as calculated by the plane wave DFT method. (a) Top view; (b) side view.

near the Fermi level, the defect-defect interaction should split the peak into two close peaks, thus opening a way for defect-mediated band-structure engineering.

Vacancy-vacancy interaction through the strain field and electronic degrees of freedom should change the migration of vacancies, especially at low temperatures. The interplay between two different vacancy-vacancy interaction mechanisms results in a complicated energy profile. When the electronic effects are weak, the interaction can be either repulsive if the overlapping strain fields are of the same sign or attractive if the vacancy orientation is different so that the fields compensate each other. Overall, the compensation of two strain fields of opposite signs near two nearby defects favors formation of divacancies from single vacancies, while electronic effects may give rise to a correlated distribution of defects, similar to adatoms on metal surfaces,⁴⁴ which can be used for engineering the local electronic structure of nanotubes with defects. We believe our results are general and are relevant for all kinds of single-walled nanotubes and multi-walled nanotubes with small diameters.

IV. CONCLUSIONS

In this work, by atomistic simulations we studied the structure and energies of large vacancy clusters and showed that, although the formation of small vacancy clusters from isolated vacancies is energetically favorable, the existence of big holes is not, as the vacancies formed by more than five missing atoms tend to split into smaller defects due to the reconstruction of the nanotube atomic network. This explains why the nanotubes irradiated at high temperatures preserve their tubular shape but contract locally,^{11,36} while at low temperatures the nanotubes are quickly destroyed. The existence of the optimum temperature for peapod formation can be understood in terms of splitting of big vacancy clusters into smaller defects, so that big holes required for the diffusion of fullerenes inside nanotubes disappear. As the network reconstruction is more efficient in small-diameter nanotubes, our results also explain experimental observations²¹ that it is easier to close holes in nanotubes with small diameters. We stress, however, that for full understanding of the reversible hole engineering in carbon nanotubes²¹ the knowledge on the energy barriers separating various configurations is required, which is beyond the scope of our work. We would also like to point out that, although big vacancy clusters are energetically unfavorable, they can appear at low temperatures due to

chemical treatment or irradiation. We also showed that electronic and mechanical effects give rise to long-range interactions between single vacancies in carbon nanotubes, which may govern the migration of vacancies, especially at low temperatures.

ACKNOWLEDGMENTS

We thank F. Banhart and P. M. Ajayan for useful discussions. Grants of computer time from the Center of Scientific Computing in Espoo, Finland are gratefully acknowledged.

- ¹Y. Fan, B. R. Goldsmith, and P. G. Collins, *Nat. Mater.* **4**, 906 (2005).
- ²M. C. Gordillo, *Phys. Rev. Lett.* **96**, 216102 (2006).
- ³G. Gómez-Navarro, P. J. De Pablo, J. Gómez-Herrero, B. Biel, F. J. García-Vidal, A. Rubio, and F. Flores, *Nat. Mater.* **4**, 534 (2005).
- ⁴N. Neophytou, D. Kienle, E. Polizzi, and M. P. Anantram, *Appl. Phys. Lett.* **88**, 242106 (2006).
- ⁵H. J. Choi, J. Ihm, S. G. Louie, and M. L. Cohen, *Phys. Rev. Lett.* **84**, 2917 (2000).
- ⁶J. A. Robinson, E. S. Snow, S. C. Bădescu, T. L. Reinecke, and F. K. Perkins, *Nano Lett.* **6**, 1747 (2006).
- ⁷M. K. Kostov, E. E. Santiso, A. M. George, K. E. Gubbins, and M. B. Nardelli, *Phys. Rev. Lett.* **95**, 136105 (2005).
- ⁸S. Zhang, S. L. Mielke, R. Khare, D. Troya, R. S. Ruoff, G. C. Schatz, and T. Belytschko, *Phys. Rev. B* **71**, 115403 (2005).
- ⁹T. Dumitrica, M. Hua, and B. I. Yakobson, *Proc. Natl. Acad. Sci. U.S.A.* **103**, 6105 (2006).
- ¹⁰M. Sannalampi, A. Krasheninnikov, A. Kuronen, K. Nordlund, and K. Kaski, *Phys. Rev. B* **70**, 245416 (2004).
- ¹¹L. Sun, F. Banhart, A. Krasheninnikov, J. A. Rodríguez-Manzo, M. Terrones, and P. Ajayan, *Science* **312**, 1199 (2006).
- ¹²M. Terrones, F. Banhart, N. Grobert, J.-C. Charlier, H. Terrones, and P. M. Ajayan, *Phys. Rev. Lett.* **89**, 075505 (2002).
- ¹³M. S. Raghuvver, P. G. Ganesan, J. D'Arcy-Gall, G. Ramanath, M. Marshall, and I. Petrov, *Appl. Phys. Lett.* **84**, 4484 (2004).
- ¹⁴A. J. Lu and B. C. Pan, *Phys. Rev. Lett.* **92**, 105504 (2004).
- ¹⁵J. Rossato, R. J. Baierle, A. Fazzio, and R. Mota, *Nano Lett.* **5**, 197 (2005).
- ¹⁶S. Berber and A. Oshiyama, *Physica B* **376-377**, 272 (2006).
- ¹⁷A. V. Krasheninnikov, P. O. Lehtinen, A. S. Foster, and R. M. Nieminen, *Chem. Phys. Lett.* **418**, 132 (2006).
- ¹⁸J. M. Carlsson, *Phys. Status Solidi B* **243**, 3452 (2006).
- ¹⁹A. J. R. da Silva (private communication).
- ²⁰S. Berber, Y.-K. Kwon, and D. Tománek, *Phys. Rev. Lett.* **88**, 185502 (2002).
- ²¹F. Hasi, F. Simon, and H. Kuzmany, *J. Nanosci. Nanotechnol.* **5**, 1785 (2005).
- ²²T. Frauenheim, G. Seifert, M. Elstner, T. Niehaus, C. Köhler, M. Amkreutz, M. Sternberg, Z. Hajnal, A. Di Carlo, and S. Suhai, *J. Phys.: Condens. Matter* **14**, 3015 (2002).
- ²³A. V. Krasheninnikov, K. Nordlund, P. O. Lehtinen, A. S. Foster, A. Ayuela, and R. M. Nieminen, *Phys. Rev. B* **69**, 073402 (2004).
- ²⁴D. W. Brenner, *Phys. Rev. B* **42**, 9458 (1990).
- ²⁵B. Ni, R. Andrews, D. Jacques, D. Qian, M. B. J. Wijesundara, Y. Choi, L. Hanley, and S. B. Sinnott, *J. Phys. Chem. B* **105**, 12719 (2001).
- ²⁶M. Huhtala, A. V. Krasheninnikov, J. Aittoniemi, S. J. Stuart, K. Nordlund, and K. Kaski, *Phys. Rev. B* **70**, 045404 (2004).
- ²⁷A. V. Krasheninnikov, K. Nordlund, and J. Keinonen, *Phys. Rev. B* **65**, 165423 (2002).
- ²⁸A. V. Krasheninnikov, K. Nordlund, M. Sirviö, E. Salonen, and J. Keinonen, *Phys. Rev. B* **63**, 245405 (2001).
- ²⁹A. V. Krasheninnikov, K. Nordlund, and J. Keinonen, *Appl. Phys. Lett.* **81**, 1101 (2002).
- ³⁰D. W. Brenner, O. A. Shenderova, J. A. Harrison, S. J. Stuart, B. Ni, and S. B. Sinnott, *J. Phys.: Condens. Matter* **14**, 783 (2002).
- ³¹G. Kresse and J. Furthmüller, *Phys. Rev. B* **54**, 11169 (1996).
- ³²P. O. Lehtinen, A. S. Foster, Y. Ma, A. V. Krasheninnikov, and R. M. Nieminen, *Phys. Rev. Lett.* **93**, 187202 (2004).
- ³³P. E. Blöchl, *Phys. Rev. B* **50**, 17953 (1994).
- ³⁴J. P. Perdew, J. A. Chevary, S. H. Vosko, K. A. Jackson, M. R. Pederson, D. J. Singh, and C. Fiolhais, *Phys. Rev. B* **46**, 6671 (1992).
- ³⁵G. D. Lee, C. Z. Wang, E. Yoon, N. M. Hwang, D. Y. Kim, and K. M. Ho, *Phys. Rev. Lett.* **95**, 205501 (2005).
- ³⁶F. Banhart, J. X. Li, and A. V. Krasheninnikov, *Phys. Rev. B* **71**, 241408(R) (2005).
- ³⁷J. M. Carlsson and M. Scheffler, *Phys. Rev. Lett.* **96**, 046806 (2006).
- ³⁸A. A. El-Barbary, R. H. Telling, C. P. Ewels, M. I. Heggie, and P. R. Briddon, *Phys. Rev. B* **68**, 144107 (2003).
- ³⁹A. Misra, M. K. Tyagi, K. Pawan, Singh, D. S. Misra, J. Ghatak, P. V. Satyam, and D. K. Avasthi, *Diamond Relat. Mater.* **15**, 300 (2006).
- ⁴⁰C. Ewels (private communication).
- ⁴¹K. M. Beardmore and N. Gronbech-Jensen, *Phys. Rev. B* **60**, 12610 (1999).
- ⁴²A. V. Krasheninnikov, *Solid State Commun.* **118**, 361 (2001).
- ⁴³Z. Osváth, G. Vértesy, L. Tapasztó, F. Wéber, Z. E. Horváth, J. Gyulai, and L. P. Biró, *Phys. Rev. B* **72**, 045429 (2005).
- ⁴⁴J. Repp, F. Moresco, G. Meyer, K.-H. Rieder, P. Hyldegaard, and M. Persson, *Phys. Rev. Lett.* **85**, 2981 (2000).
- ⁴⁵A. V. Krasheninnikov *et al.* (unpublished).